Characterization of Molecular Orientation in Polyethylene by Raman Spectroscopy

Marie Pigeon, Robert E. Prud'homme, and Michel Pézolet*

Centre de Recherche en Sciences et Ingénierie des Macromolécules, Département de Chimie, Université Laval, Cité Universitaire, Québec, Canada G1K 7P4

Received February 11, 1991; Revised Manuscript Received May 15, 1991

ABSTRACT: The polarization dependences of several Raman bands of roll-drawn high-density polyethylene of uniaxial symmetry were investigated at different draw ratios between 7.0 and 11.7. When the right-angle scattering geometry was used, it was possible to determine quantitatively the principal components of the Raman tensors of the 1080-, 1130-, and 1170-cm^{-1} vibrations. The orientation coefficients $\langle P_2(\cos\theta)\rangle$ and $\langle P_4(\cos\theta)\rangle$ of the C–C bonds with trans conformation and gauche defects were also calculated by using these bands. The results obtained from the 1080-cm^{-1} band show that the orientation of gauche structures does not vary much with the draw ratio (between 7.0 and 11.7). On the other hand, the polarization behavior of the 1130-cm^{-1} band indicates that trans conformers in the amorphous phase orient more readily in the draw direction. When the components of the Raman tensors obtained from right-angle scattering were used, it was found that backscattering measurements could yield good estimates of $\langle P_2(\cos\theta)\rangle$ and $\langle P_4(\cos\theta)\rangle$ orientation averages. Finally, a method is proposed for the rapid evaluation of these parameters from calibration curves obtained from backscattering spectra measured with the polarization direction of both the incident and scattered light parallel to the draw direction. This method should be particularly useful for the determination of the distribution of the orientation of trans bonds in thick processed samples of polyethylene.

Introduction

In order to take full advantage of the intrinsic stiffness of polymer chains, attempts have been made to orient them as much as possible, leading to the production of high-modulus fibers and films. High-density polyethylene is one of the polymers that has been used for that purpose. Its industrial importance has created a need to develop methods to characterize its degree of orientation and uniformity through thick sections.

The orientation of semicrystalline polymers has been investigated by various experimental methods such as birefringence, X-ray diffraction and scattering techniques, fluorescence polarization, nuclear magnetic resonance spectroscopy, sonic modulus, and vibrational spectroscopy.[1-3] Raman and infrared spectroscopies provide methods for the independent determination of the molecular orientation of both the crystalline and amorphous phases of semicrystalline polymers. Raman scattering has, however, some advantages over infrared spectroscopy. First, it enables the determination of both the second and fourth terms, $\langle P_2(\cos\theta)\rangle$ and $\langle P_4(\cos\theta)\rangle$, respectively, of the expansion of the orientation distribution function. These parameters are necessary to fully define the orientation function of oriented polymers[1,2] and to understand the mechanical properties of polymers in terms of models. Second, for orientation determination, Raman spectroscopy does not require the use of thin polymer films, as for infrared absorption measurements.

However, since orientation determination by Raman spectroscopy is more complex than that by infrared spectroscopy from both experimental and theoretical points of view, only a few quantitative measurements have been performed so far. Besides the approach of Cornell and Koenig[4] and that of Snyder,[5] who have considered rather special distributions of orientation, Bower[6] has developed a general theory for the quantitative determination of the degree of molecular orientation of polymers from their polarized Raman spectra. So far, this method has been applied satisfactorily to poly(methyl methacrylate),[7] polyethylene,[8] polypropylene,[9] poly(vinyl chloride),[10] polystyrene,[11] and poly(ethylene terephthalate).[12-14]

Oriented polyethylene has been the object of several Raman investigations, most of them being related to the assignments of the Raman active modes[15-18] or to the determination of its crystallinity.[19] On the other hand, in order to obtain information on the all-trans chain-length distribution, Snyder et al.[20] and Wang et al.[21] have followed the changes in the low-frequency Raman longitudinal acoustic modes of a high-density polyethylene. In addition, Maxfield et al.[8] have determined the molecular orientation of the crystalline and amorphous phases of thin films of oriented low-density polyethylene using Bower's method.[6]

In the present study, Raman spectroscopy has been used to determine quantitatively the chain orientation in thick samples of oriented high-density polyethylene, using different Raman active modes. In addition, it is shown that when the components of the Raman tensor of a given band are known from right-angle measurements, backscattering results can yield accurate values of $\langle P_2(\cos\theta)\rangle$ and $\langle P_4(\cos\theta)\rangle$. Finally, we propose a method for rapid evaluation of these parameters from the polarized Raman spectrum measured with the polarization direction of both incident and scattered light parallel to the draw direction.

Theory

Bower[6] has developed a procedure for the determination of the distribution of orientation of polymer chains by polarized Raman scattering. This method is based on previous studies by Roe,[22] who used a series of generalized spherical harmonics to describe the distribution of the Euler angles defining the orientation, with respect to reference axes, of sets of rectangular coordinate axes fixed within orientable units. For representing the polymer network, Treloar's[23] model is used, in which each chain, that is, the portion of a polymer molecule connecting two successive cross-link points, consists of a certain number of freely jointed statistical segments.

As mentioned by Bower,[6] the Raman scattering intensity, I_s, is given by a quadratic expression of all components

* Author to whom correspondence should be addressed.

0024-9297/91/2224-5687$02.50/0

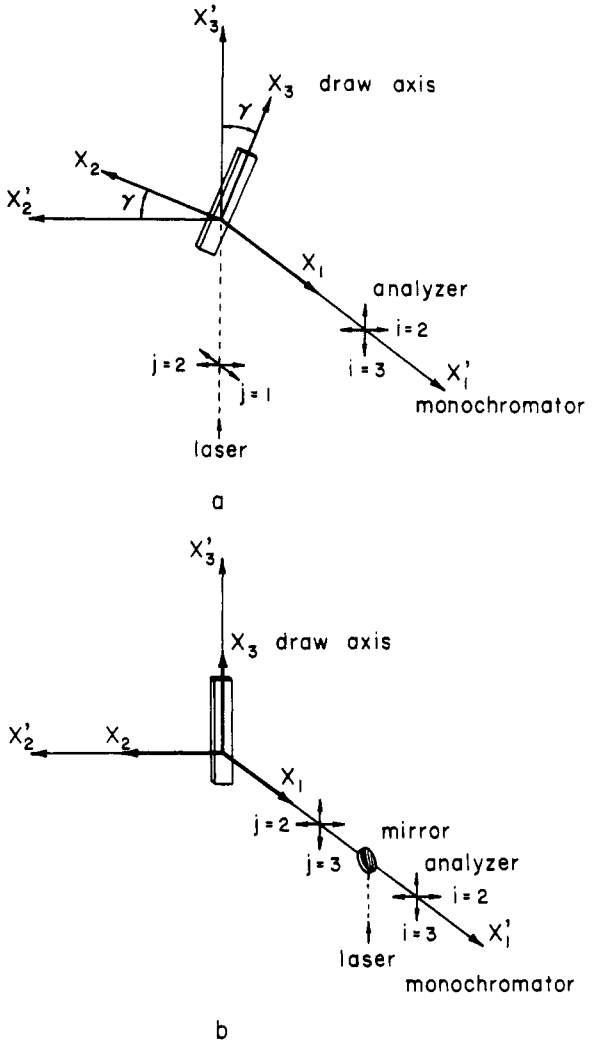

Figure 1. Experimental arrangement and coordinate axes for (a) right-angle and (b) backscattering Raman geometries.

of the Raman tensor for the vibration studied, α_{ij} (i, j = 1–3), the coefficients being the directions cosines I_i and I_j' defining, respectively, the polarization direction of the incident and scattered light with respect to a set of axes O–X_1,X_2,X_3 fixed in the sample

$$I_s = I_0 \sum (\sum_{ij} I_i I_j' \alpha_{ij})^2 \quad (1)$$

where I_0 is a constant depending on instrumental factors and the incident light intensity. The experimental values are thus of the form $I_0 \sum \alpha_{ij}\alpha_{pq}$, and since the summation implies that all the scattering units contributing to the observed intensity are considered, they contain information about the distribution of orientation of these units. Each α_{ij} can be expressed as a linear combination of the principal components α_1, α_2, and α_3 of the derived polarizability or Raman tensor of the vibration investigated and the Euler angles defining the orientation of the principal axes of the tensor with respect to axes O–X_1,X_2,X_3 of the sample.

In the case of uniaxial statistical symmetry, with no preferred orientation around the chain axis O–x_3 and when the tensor axes are coincident with the structural units axes O–x_1,x_2,x_3, we have

$$\sum \alpha_{ij}\alpha_{pq} = 4\pi^2 N_0 \sum_l M_{l00} A_{l00}^{ijpq} \quad (2)$$

where N_0 is the number of structural units contributing to the Raman intensity and A_{l00}^{ijpq} a sum of quadratic terms in α_1, α_2, and α_3, previously tabulated by Bower.[6] M_{l00} is expressed in terms of Legendre polynomials $\langle P_l(\cos\theta)\rangle$ by

$$M_{l00} = 1/4\pi^2((2l+1)/2)^{1/2}\langle P_l(\cos\theta)\rangle \quad (3)$$

with $\langle P_l(\cos\theta)\rangle$ the coefficient of the lth term in the expansion of the orientation distribution function for the set of symmetry axes O–x_1,x_2,x_3 of the structural units with respect to the sample axes O–X_1,X_2,X_3; θ is the angle between the O–x_3 chain axis of the structural units and the O–X_3 axis fixed in the sample, that is, the stretching direction. It follows from eq 3 that

$$M_{000} = 1/4\pi^2(1/2)^{1/2} \quad (4)$$

$$M_{200} = 1/4\pi^2(5/2)^{1/2}\langle P_2(\cos\theta)\rangle \quad (5)$$

$$M_{400} = 1/4\pi^2(9/2)^{1/2}\langle P_4(\cos\theta)\rangle \quad (6)$$

For a sample with uniaxial symmetry, there are only five independent nonzero sums $\sum \alpha_{ij}\alpha_{pq}$ that are of the form $\sum \alpha_{ii}\alpha_{jj}$ or $\sum \alpha_{ij}^2$. The expressions of the experimental Raman scattering intensity for each of these $\sum \alpha_{ij}\alpha_{pq}$, for a vibration with its tensor axes coincident with the structural unit axes, are thus

$$I_0\sum \alpha_{22}^2 = b[(3a_1^2 + 3a_2^2 + 3 + 2a_1a_2 + 2a_1 + 2a_2)/15 + P_2(3a_1^2 + 3a_2^2 - 6 + 2a_1a_2 - a_1 - a_2)/21 + 3P_4(3a_1^2 + 3a_2^2 + 8 + 2a_1a_2 - 8a_1 - 8a_2)/280] \quad (7)$$

$$I_0\sum \alpha_{33}^2 = b[(3a_1^2 + 3a_2^2 + 3 + 2a_1a_2 + 2a_1 + 2a_2)/15 - 2P_2(3a_1^2 + 3a_2^2 - 6 + 2a_1a_2 - a_1 - a_2)/21 + P_4(3a_1^2 + 3a_2^2 + 8 + 2a_1a_2 - 8a_1 - 8a_2)/35] \quad (8)$$

$$I_0\sum \alpha_{21}^2 = b[(a_1^2 + a_2^2 + 1 - a_1a_2 - a_1 - a_2)/15 + P_2(a_1^2 + a_2^2 - 2 - 4a_1a_2 + 2a_1 + 2a_2)/21 + P_4(3a_1^2 + 3a_2^2 + 8 + 2a_1a_2 - 8a_1 - 8a_2)/280] \quad (9)$$

$$I_0\sum \alpha_{32}^2 = b[(a_1^2 + a_2^2 + 1 - a_1a_2 - a_1 - a_2)/15 - P_2(a_1^2 + a_2^2 - 2 - 4a_1a_2 + 2a_1 + 2a_2)/42 - P_4(3a_1^2 + 3a_2^2 + 8 + 2a_1a_2 - 8a_1 - 8a_2)/70] \quad (10)$$

$$I_0\sum \alpha_{22}\alpha_{33} = b[(a_1^2 + a_2^2 + 1 + 4a_1a_2 + 4a_1 + 4a_2)/15 - P_2(a_1^2 + a_2^2 - 2 + 10a_1a_2 - 5a_1 - 5a_2)/42 - P_4(3a_1^2 + 3a_2^2 + 8 + 2a_1a_2 - 8a_1 - 8a_2)/70] \quad (11)$$

By solving these five nonlinear equations iteratively, the five unknowns, which are b ($=I_0N_0\alpha_3^2$), a_1 ($=\alpha_1/\alpha_3$), a_2 ($=\alpha_2/\alpha_3$), P_2 ($=\langle P_2(\cos\theta)\rangle$), and P_4 ($=\langle P_4(\cos\theta)\rangle$), can be determined.

Experimental Section

Samples used for this study were roll-drawn sheets of high-density polyethylene (HDPE) prepared by Dr. Raymond Woodhams of the University of Toronto. X-ray diffraction measurements have shown that these samples were uniaxially oriented.[24] They had draw ratios (λ) between 7 and 11.7, with a thickness of about 1 mm (0.8–1.2 mm). Densities were determined in a density gradient column, at room temperature, in a diethylene glycol/isopropyl alcohol mixture.

The Raman spectra were recorded with a Spex Model 1400 double-monochromator computerized spectrometer using a Spectra Physics Model 2020 argon ion laser tuned at 514.5 nm.[25]

Experiments were done by using both 90° and 180° scattering geometries. In the former case (Figure 1a), the exciting beam was incident on the edge of the sample along the $O-X_3'$ direction of a system of axes $O-X_1',X_2',X_3'$ fixed in the laboratory, and the scattered light was collected at a right angle along the $O-X_1'$ axis. The polarization of the linearly polarized incident radiation was set parallel to either $O-X_1'$ or $O-X_2'$, using a half-wave plate, while that of the analyzer was parallel to $O-X_2'$ or $O-X_3'$. The specimen was positioned so that the $O-X_1$ axis fixed in the sample was always coincident with the $O-X_1'$ axis of the laboratory, the axis $O-X_3$ making an angle γ with $O-X_3'$. For each angle γ used, four scattered intensities $I_{ij}(\gamma)$ can be defined, with the polarization of the incident light parallel to the $O-X_j'$ (j = 1 or 2) direction and with the polarization of the scattered light parallel to the $O-X_i'$ (i = 2 or 3) direction (Figure 1a). Inserting the appropriate values of the direction cosines into eq 1, we have

$$I_{21}(\gamma) = I_0\sum(\alpha_{21}\cos\gamma - \alpha_{31}\sin\gamma)^2 \quad (12)$$

$$I_{31}(\gamma) = I_0\sum(\alpha_{21}\sin\gamma - \alpha_{31}\cos\gamma)^2 \quad (13)$$

$$I_{22}(\gamma) = I_0\sum(\alpha_{22}\cos^2\gamma - \alpha_{32}\sin 2\gamma + \alpha_{33}\sin^2\gamma)^2 \quad (14)$$

$$I_{32}(\gamma) = I_0\sum(1/2\alpha_{22}\sin 2\gamma + \alpha_{32}\cos^2\gamma - \alpha_{32}\sin^2\gamma - 1/2\alpha_{33}\sin 2\gamma)^2 \quad (15)$$

Using γ values of 0°, 45°, and 90° in order to simplify as much as possible the equations, we have all the experimental measurements required to solve the set of eqs 7–11.

For the backscattering (180°) geometry (Figure 1b), a small mirror was placed in the laser path to reflect the exciting beam perpendicularly to the polyethylene sheet ($O-X_1$ axis), and the scattered light was collected at approximately 180° from this direction, along the $O-X_1'$ axis. The polarization of both the incident light and the analyzer was parallel to the $O-X_2'$ or $O-X_3'$ axes of the laboratory. For these experiments, the sample was fixed so that its set of axes $O-X_1,X_2,X_3$ was always coincident with the set $O-X_1',X_2',X_3'$ of the laboratory. The intensities $I_{ij}(\gamma=0°)$ observed when the polarization of the incident light is parallel to the $O-X_j'$ (j = 2 or 3) direction and when the polarization of the scattered light is parallel to the $O-X_i'$ (i = 2 or 3) direction then take the following values:

$$I_{22} = I_0\sum\alpha_{22}^2 \quad (16)$$

$$I_{23} = I_{32} = I_0\sum\alpha_{32}^2 \quad (17)$$

$$I_{33} = I_0\sum\alpha_{33}^2 \quad (18)$$

For both scattering geometries, the scattered light was collected with a $f/2$ lens and the parallel beam was focused on the entrance slit of the monochromator with a $f/5$ lens. An analyzer and a polarization scrambler were positioned between the second lens and the monochromator. All spectra were obtained at approximately 21 °C, with 100-mW laser power at the sample, at a spectral resolution of 5 cm^{-1}, and with an integration period of 2 s by a 2-cm^{-1} step. Samples were mounted on a rotator–translator stage for precise positioning. In order to minimize the polarization scrambling by the sample for the right-angle scattering geometry, the exciting beam was focused just below the surface of the material, and the scattered light was collected after passing through a very thin layer of the polymer. In addition, backscattering spectra obtained from 10-μm films microtomed from the samples were identical with the spectra obtained with the thick samples. The absence of depolarization of the scattered light by the sample was also checked from the $I_0\sum\alpha_{32}^2$ spectra observed with γ = 0° or 90°. The intensity of these spectra must be equal when the polarization of the incident light (and of the scattered light for γ = 90°) is rotated by 90°. For γ = 45°, the birefringence has more effect on the scattered radiation, and it was difficult to verify that no scrambling effect took place because the spectra in this orientation are always the sum of more than one $I_0\sum\alpha_{ij}\alpha_{pq}$ terms. According to Bower,[6] it seems that these errors are difficult to eliminate.

Table I
Assignments of the Raman Bands of Polyethylene[a]

frequency, cm^{-1}	phase	mode	symmetry
1060	C (A)	ν_{as}(C–C)	$B_{2g} + B_{3g}$
1080	A	ν(C–C)	
1130	C (A)	ν_s(C–C)	$A_g + B_{1g}$
1170	C (A)	$\rho(CH_2)$	$A_g + B_{1g}$
1296	C	$\tau(CH_2)$	$B_{2g} + B_{3g}$
1310	A		
1370	C	$\omega(CH_2)$	$B_{2g} + B_{3g}$
1418	C	$\delta(CH_2)$	A_g
1440	A	Fermi resonance + overtones?	$B_{1g} + A_g$?
1460	A		$A_g + B_{1g}$?

[a] C, crystalline; A, amorphous; ν, stretching (s, symmetric; as, asymmetric); ρ, rocking; δ, bending; τ, twisting; ω, wagging.

Results and Discussion

Assignment of the Raman Bands. In order to obtain information about the distribution of molecular orientation from Raman intensities, it is very important to know the structure of the molecular chain and the assignment of the Raman lines. The main features in the Raman spectrum of polyethylene in the 1000–1500-cm^{-1} region are listed in Table I along with their assignment based on previous Raman studies on orthorhombic polyethylene.[15-18,26-28] As seen in this table, the orientation of both the crystalline and amorphous phases of polyethylene can be determined from different Raman bands.

In the crystals, the carbon skeleton of the chains has a planar zigzag structure, the C–C bonds being in the all-trans conformation. On the other hand, in the amorphous phase of the polymer, the chain conformation is not anymore uniform and is composed of different sequences of trans and gauche bonds.

In order to simplify the mathematical analysis of the Raman data, only the vibrations with their tensor axes coincident with the axes of the structural units will be considered. Only the modes with A_g and B_{1g} symmetry fill this requirement, and the B_{2g} or B_{3g} modes will not be analyzed.

The in-phase skeletal stretching vibration of the C–C bonds of the extended polyethylene molecule occurs at 1130 cm^{-1} and has the symmetry properties of both A_g and B_{1g} species. It is interesting to note that the calculated normal-mode frequency of a single chain is approximately the same.[29] Also, normal-mode calculations on *n*-paraffins have shown that C–C skeletal vibrations are highly delocalized and that the frequency of this C–C stretching vibration for molecules having one or two gauche bonds is the same as that of the fully extended molecule.[30] Therefore, the intensity of the 1130-cm^{-1} band is associated with all-trans C–C bonds, whether these bonds are located in the crystalline or the amorphous phases.

The 1080-cm^{-1} band has been assigned to the stretching of the C–C skeleton of different kinds of gauche structures.[30,31] It primarily arises from the amorphous part of the polymer and from the folds between adjacent planar zigzag sequences in the crystalline phase and has been used by Maxfield et al.[8] for the measurement of the orientation of the amorphous phase. For highly oriented polyethylene, such as the samples used in the current study, the intensity of this band is very low (Figure 2), due to the high crystallinity of the samples.

The band at 1170 cm^{-1} has also the $A_g + B_{1g}$ symmetry and results from the CH_2 rocking mode. As for the 1130-cm^{-1} feature, this band comes mostly from the

crystalline part of the polymer, but the trans C–C bonds in the amorphous phase are also expected to contribute to the scattering intensity at this frequency. Maxfield et al.[8] have used this band to calculate the orientation of the crystalline part of samples of low-density polyethylene. It is clearly visible in the Raman spectra of the sample used (Figure 2), but, for certain polarizations, it is almost completely extinguished.

The origin of the bands due to the CH_2 bending modes of polyethylene around 1450 cm^{-1} is more ambiguous because of the possibility of Fermi resonance between the Raman active CH_2 bending modes and the first overtones and the possible combinations of the infrared active CH_2 rocking modes.[15,28] Nevertheless, it has been shown that, for orthorhombic polyethylene, which contains two structural units per unit cell, factor group splitting of the CH_2 mode results in two components at 1418 and 1440 cm^{-1}.[32] The 1418-cm^{-1} band is well separated from the other components of this spectral region and has been used successfully to determine the crystallinity of polyethylene.[19] On the other hand, the remaining peaks of the band system are not easily assigned, even for the highly crystalline polymer. Luu et al.[33,34] have suggested a new assignment for this spectral region based on a three-phase model. They have proposed the coexistence of melted and solid amorphous phases characterized by broad bands at 1460 and 1440 cm^{-1}, respectively. The former can be represented by a sort of random coil with several gauche bonds while the latter consists of an assembly of chains mainly of the trans conformation but lacking the regular packing of the crystalline phase. The third phase is the orthorhombic crystalline phase characterized by the 1418-cm^{-1} band. Attempts will be made to calculate the orientation of both crystalline and amorphous phases from this band system.

Intensity Determination. The intensity of the bands at 1130 and 1170 cm^{-1} was determined directly from peak height measurements since these bands do not overlap significantly with other spectral features. However, in the case of the 1080-cm^{-1} band, it was necessary to decompose the 1000–1250-cm^{-1} region into four components (1060, 1080, 1130, and 1170 cm^{-1}) by using the method of Pitha and Jones[35] and the Gauss–Lorentz sum function (50–80% Lorentz) since its intensity was very low due to the high crystallinity of the samples used. The frequency and the width at half-height of the 1080-cm^{-1} band were first determined from the $I_0\sum\alpha_{22}^2$ spectrum since the band is stronger for this spectrum, and these spectral parameters were held fixed for the other spectra. The intensity of each component was measured either from the peak height or the area under the peak. For the 1400–1500-cm^{-1} region, it was possible to make a rather good estimation of the height of the three bands, but again a decomposition (60–85% Lorentz) of this spectral region was necessary to obtain reliable measurements.

In order to be able to determine from right-angle Raman scattering the five independent $I_0\sum\alpha_{ij}\alpha_{pq}$ values needed to calculate the second and fourth terms of the expansion of the orientation distribution, it is necessary to record spectra with three different orientations of the sample relative to the direction of the laser beam (angle γ in Figure 1). Therefore, the angle γ was successively adjusted to 0°, 45°, and 90°. For a series of four spectra at a given γ angle, the only intensity correction was the difference of the intensity of the exciting radiation with different polarizations. The normalization between series of spectra obtained at different γ angles was done from spectra giving the same $I_0\sum\alpha_{ij}\alpha_{pq}$ or a combination of them.

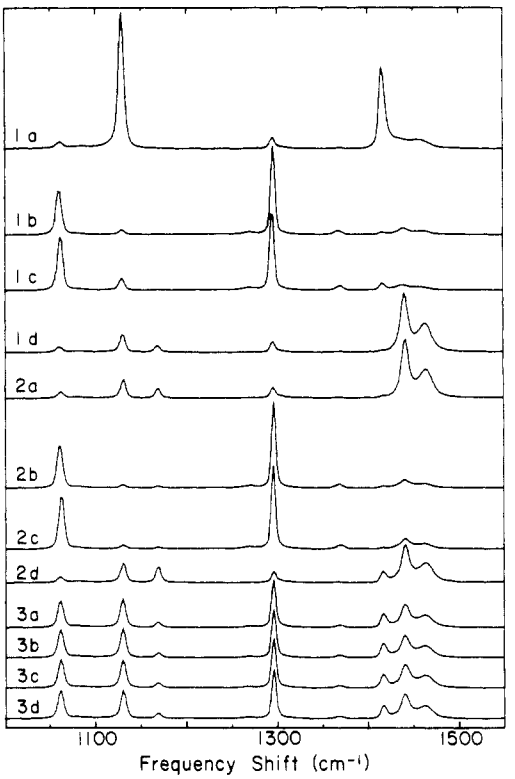

Figure 2. Polarized Raman spectra of polyethylene (draw ratio of 11.7) obtained by using the right-angle scattering geometry with (1) $\gamma = 90°$, (2) $\gamma = 0°$, and (3) $\gamma = 45°$. Each spectrum is related to the following intensity parameters: 1a = $I_0\sum\alpha_{33}^2$; 1b, 1c, 2b, and 2c = $I_0\sum\alpha_{32}^2$; 1d and 2a = $I_0\sum\alpha_{21}^2$; 2d = $I_0\sum\alpha_{22}^2$; 3a = $I_0\sum[(\alpha_{22}^2 + \alpha_{33}^2)/4 + \alpha_{22}\alpha_{33}/2 + \alpha_{23}^2]$; 3b = $I_0\sum[(\alpha_{22}^2 + \alpha_{33}^2)/4 - \alpha_{22}\alpha_{33}/2]$; 3c and 3d = $I_0\sum(\alpha_{21}^2 + \alpha_{32}^2)/2$.

Spectra were first normalized, as shown in Figure 2, for a sample with a draw ratio of 11.7, and the spectra for the same $I_0\sum\alpha_{ij}\alpha_{pq}$ were averaged in order to improve the accuracy of the measurements and to minimize birefringence effects. Since it is not possible to measure directly the $I_0\sum\alpha_{22}\alpha_{33}$ spectrum, it was calculated from other spectra. This spectrum is therefore less accurate, especially since birefringence problems are likely to occur at this sample position ($\gamma = 45°$). The five independent $I_0\sum\alpha_{ij}\alpha_{pq}$ normalized spectra are shown in Figure 3 for the $\lambda = 11.7$ sample, and the intensities of the bands investigated for samples of PE stretched at $\lambda = 7$ and 11.7 are reported in Table II where the intensity of the strongest band was adjusted to 1. All values were obtained from the integrated intensities, although very similar results were also obtained from peak height measurements.

Orientation Parameters and Raman Tensors. With the five independent $I_0\sum\alpha_{ij}\alpha_{pq}$ values obtained for each band, the second and fourth terms of the expansion of the distribution function were calculated. Initial starting values and limits for each unknown were necessary for the iterative least-squares program to solve the set of eqs 7–11. The "b" parameter, which depends on instrumental factors and the incident light intensity, is always positive. Since the samples studied were highly oriented, the initial value for $\langle P_2(\cos\theta)\rangle$ was set close to unity, and, accordingly, the $\langle P_4(\cos\theta)\rangle$ value was chosen as the most probable one.[36] It was more difficult to estimate the initial value of the unknown a_1 and a_2, corresponding to the ratios of the principal components of the Raman tensor, α_1/α_3 and α_2/α_3, respectively, for a given vibrational mode. Nevertheless, from the atomic displacements for each vibration, it was possible to make an assumption of their relative sign and amplitude. It is important to keep in mind that more

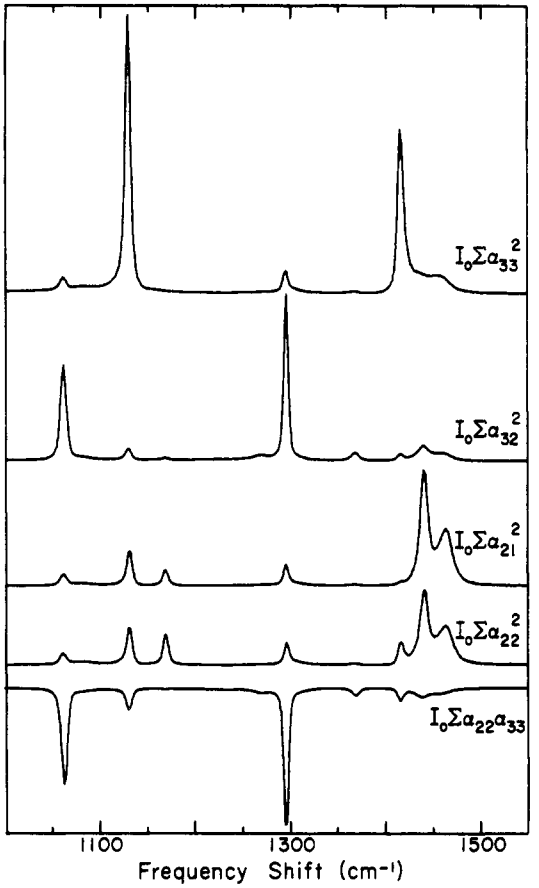

Figure 3. Five independent $I_0\sum\alpha_{ij}\alpha_{pq}$ normalized spectra used for orientation determination of polyethylene (draw ratio of 11.7).

Table II
Relative Intensities[a] of the Raman Bands for the Different $I_0\sum\alpha_{ij}\alpha_{pq}$

frequency, cm^{-1}	λ	$I_0\sum\alpha_{22}^2$	$I_0\sum\alpha_{33}^2$	$I_0\sum\alpha_{12}^2$	$I_0\sum\alpha_{23}^2$	$I_0\sum\alpha_{22}\alpha_{33}$
1080	7	0.702	1.000	0.485	0.214	−0.20
	11.7	0.653	1.000	0.462	0.178	−0.20
1130	7	0.150	1.000	0.120	0.079	−0.08
	11.7	0.157	1.000	0.142	0.050	−0.05
1170	7	1.000	0.002	0.406	0.109	−0.12
	11.7	1.000	0.001	0.531	0.101	−0.10
1418	7	0.190	1.000	0.027	0.059	−0.06
	11.7	0.120	1.000	0.018	0.030	−0.03
1440	7	0.906	0.106	1.000	0.195	−0.20
	11.7	0.739	0.302	1.000	0.189	−0.20
1460	7	0.859	0.412	1.000	0.259	−0.30
	11.7	0.685	0.294	1.000	0.135	−0.10

[a] The relative intensities were calculated from the integrated intensity of each band relative to the highest value.

than one solution is possible for the nonlinear set of eqs 7–11 and that a good knowledge of the system is essential.

The results of the calculations are given in Table III for the major peaks of the 1000–1250-cm^{-1} region. As can be seen, the Raman tensor is not cylindrical for either of the vibrations investigated, as expected from the planar zigzag structure of polyethylene. Furthermore, the sign difference between the α_1/α_3 and α_2/α_3 ratios demonstrates that the polarizability changes during the vibrations have opposite sign in the plane or perpendicular to the plane of the chains. This is particularly true for the band due to the CH_2 rocking mode at 1170 cm^{-1}, since, for this vibration, the hydrogen atoms of the methylene groups move out of the plane of the chains.

As expected, the best fit for the numerical solution of eqs 7–11 was obtained for the 1130-cm^{-1} band since the intensity of this strong and well-resolved band was determined with more accuracy, and also because it is very likely that the Raman tensor coincides with the chain axis for this vibration that involves the symmetric breathing of the carbon skeleton of the polymer. Moreover, the values of the ratios α_1/α_3 and α_2/α_3 obtained from the λ = 7 and 11.7 samples using the 1130-cm^{-1} band are in excellent agreement. The value obtained for $\langle P_2(\cos\theta)\rangle$ from this band increases with the draw ratio but is always lower than that obtained by X-ray diffraction for the crystalline phase (Table IV).[24] This difference confirms the assignment of the 1130-cm^{-1} band to trans C–C bonds that are not only located in the crystalline phase. The value obtained for $\langle P_4(\cos\theta)\rangle$ falls within the range of the most probable ones.[36]

Table III
Ratios of the Principal Components of the Raman Tensors for the 1080-, 1130-, and 1170-cm^{-1} Bands of Polyethylene and Corresponding Orientation Coefficients

frequency, cm^{-1}	λ	α_1/α_3	α_2/α_3	$\langle P_2(\cos\theta)\rangle$	$\langle P_4(\cos\theta)\rangle$
1080	7	−1.10	0.79	0.42	0.40
	11.7	−1.05	0.80	0.47	0.47
1130	7	−0.54	0.31	0.75	0.56
	11.7	−0.57	0.42	0.85	0.69
1170	7	−6.2	0.42	0.84	0.45
	11.7	−7.3	0.40	0.87	0.52

Table IV
$\langle P_2(\cos\theta)\rangle$ and $\langle P_4(\cos\theta)\rangle$ for the Trans C–C Bonds of Polyethylene in the Crystalline and Amorphous Phases Determined from the 1130-cm^{-1} Band

$\langle P_n(\cos\theta)\rangle$		λ = 7	λ = 11.7
$\langle P_2(\cos\theta)\rangle_{\text{trans total}}$	Raman	0.75	0.85
$\langle P_4(\cos\theta)\rangle_{\text{trans total}}$		0.56	0.69
$\langle P_2(\cos\theta)\rangle_{\text{trans cryst}}$	X-ray[a]	0.95	0.96
$\langle P_4(\cos\theta)\rangle_{\text{trans cryst}}$		0.87	0.94
$\langle P_2(\cos\theta)\rangle_{\text{trans amorph}}$	Raman	0.27	0.60
$\langle P_4(\cos\theta)\rangle_{\text{trans amorph}}$		−0.15	0.11

[a] From ref 24.

The weakness of the 1170-cm^{-1} band introduces some nonnegligible errors of intensity, and the numerical fit for this band was not as good as that for the 1130-cm^{-1} band. Therefore, the results presented in Table III for this band are less reliable. Nevertheless, the ratios α_1/α_3 and α_2/α_3 are in fairly good agreement for the two samples investigated. As seen in Table III, the orientation averages calculated from this band are higher than those obtained from the 1130-cm^{-1} band but are also smaller than the orientation averages determined by X-ray diffraction. Therefore, neither the 1170-cm^{-1} band nor the 1130-cm^{-1} band can be used to determine the orientation of the crystalline phase of polyethylene.

The orientation of the gauche structures in the amorphous phase of the polymer was also determined by using the 1080-cm^{-1} band. Figure 2 shows that this band is weak in all spectra, and, as mentioned above, its intensity was determined from the band decomposition of the 1000–1250-cm^{-1} region. In spite of the imprecision resulting from the weakness of this band, the values obtained for $\langle P_2(\cos\theta)\rangle$ are reasonable for the amorphous phase, and the ratios α_1/α_3 and α_2/α_3 are the same for the two samples. The orientation of the gauche structures does not vary much with the draw ratio, in agreement with the infrared results of Kaito et al.[37] The values of $\langle P_4(\cos\theta)\rangle$ obtained from the 1080-cm^{-1} band are slightly too high, but they are within acceptable limits.[36]

Several attempts have been made to determine the orientation averages $\langle P_2(\cos\theta)\rangle$ and $\langle P_4(\cos\theta)\rangle$ from the bands due to the CH_2 bending modes at 1418, 1440, and

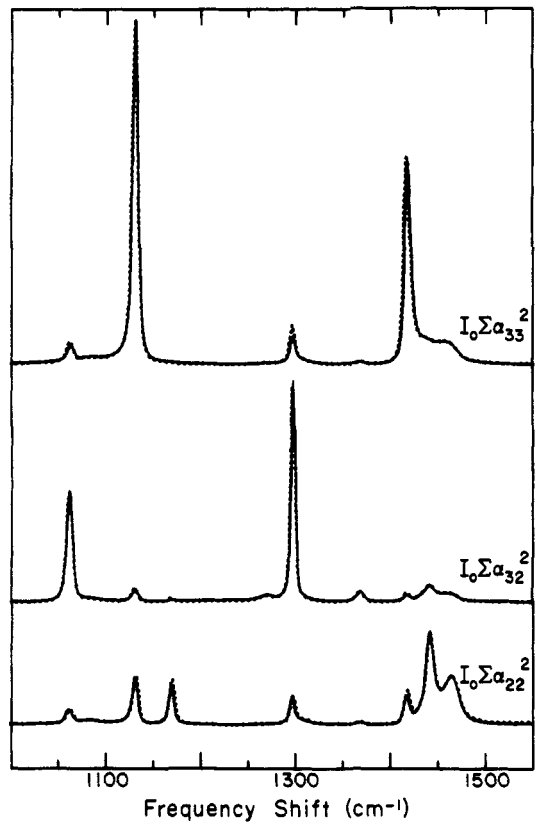

Figure 4. Comparison between right-angle (—) and backscattering (- - -) Raman spectra of polyethylene (draw ratio of 11.7).

1460 cm^{-1}. According to the three-phase model by Luu et al.,[33,34] the modes associated with these bands should have their Raman tensor axes coincident with those of the structural units. Unfortunately, even after changing the starting values of the unknowns and the intensity measurement procedure, it was not possible to solve eqs 7–11 for either of the three bands in this region. Even when the value of $I_0\sum\alpha_{22}\alpha_{33}$, which is more subjected to experimental errors, was calculated from the depolarization ratio of the Raman bands, as suggested by Maxfield et al.,[8] no solution was found for any bands of the 1400–1500-cm^{-1} region.

This result is surprising, especially for the 1418-cm^{-1} band, since it has always been associated with a mode of A_g symmetry for the orthorhombic crystalline phase of polyethylene[19,32-34] and is even used for the determination of the degree of crystallinity of polyethylene.[19] Therefore, it seems that the assignment of this spectral region is not as simple as that proposed by Luu et al.[33,34] Even though Fermi resonance is not believed to affect the intensity of the 1418-cm^{-1} band,[19] the problems encountered for the calculations of $\langle P_2(\cos\theta)\rangle$ and $\langle P_4(\cos\theta)\rangle$ most likely result from the occurrence of Fermi interactions between the Raman active CH_2 bending modes and the first overtones and the possible combination of the infrared active CH_2 rocking modes of the crystalline phase of the polymer.[15,27] It is well-known that Fermi resonance can lead to strong intensity changes due to the mixing of the vibrational wavefunctions and can affect the polarization properties of the bands involved.

At this point, it is interesting to compare the results obtained in this paper for the orientation of the trans C–C bonds from the 1130-cm^{-1} band with those of the X-ray orientation of the crystalline phase ($\langle P_n(\cos\theta)\rangle_{\text{trans cryst}}$), which is composed of chains in the all-trans conformation. As seen in Table IV, the orientation coefficients determined by X-ray diffraction are significantly higher than those obtained from the 1130-cm^{-1} Raman band, $\langle P_n(\cos\theta)\rangle_{\text{trans total}}$. This is not surprising since, as discussed above, the 1130-cm^{-1} band arises frm the C–C symmetric stretching vibration of trans bonds in both the crystalline and amorphous phases. In fact, it has been shown by Strobl and Hagedorn[19] that the Raman spectrum of semicrystalline polyethylene can be described as a superposition of three components, which originate from the orthorhombic crystalline phase, a meltlike amorphous phase, and a disordered phase of anisotropic nature where the chains are stretched but have lost their lateral order. From this model, the C–C bonds with trans conformation would be primarily located in the crystalline and anisotropic-disordered phases. Even though the method of Strobl and Hagedorn[19] has been successfully applied to the study of the morphological structure of polyethylene[38,39] and copolymers of ethylene and 1-alkenes,[40] we have not yet been able to extend it to oriented polyethylene samples since Raman spectra of randomly oriented samples are necessary for the determination of the relative amount of the three phases. Therefore, in order to be able to compare the Raman and X-ray results, we have used the more simple two-phase model, which describes the structure of polyethylene as consisting of a crystalline and an amorphous phase.

When this two-phase model is used, the orientation coefficients determined by Raman spectroscopy from the 1130-cm^{-1} band should be weighted averages of the orientation coefficients determined by X-ray diffraction and those of the trans C–C bonds in the amorphous phase, $\langle P_n(\cos\theta)\rangle_{\text{trans amorph}}$:

$$\langle P_n(\cos\theta)\rangle_{\text{trans total}} = y_{\text{cryst}}\langle P_n(\cos\theta)\rangle_{\text{trans cryst}} + (1 - y_{\text{cryst}})\langle P_n(\cos\theta)\rangle_{\text{trans amorph}} \quad (19)$$

where y_{cryst} is the weight fraction crystallinity. The latter was found from density measurements to be equal to 0.70 for the two samples used.

The results obtained from eq 19 (Table IV) reveal that, for the sample with a draw ratio of 7, the trans bonds in the amorphous phase are not highly oriented, even though the crystals are almost perfectly oriented ($\langle P_2(\cos\theta)\rangle_{\text{trans cryst}}$ close to 1). In addition, the negative value of $\langle P_4(\cos\theta)\rangle_{\text{trans amorph}}$ indicates that the distribution of the trans bonds in the amorphous phase is not centered along the draw direction. For the $\lambda = 11.7$ sample, the value of $\langle P_2(\cos\theta)\rangle_{\text{trans cryst}}$ is almost the same as that for the $\lambda = 7$ sample, but the higher value of $\langle P_4(\cos\theta)\rangle_{\text{trans cryst}}$ shows that the distribution of the crystal orientation is narrower at higher draw ratios. On the other hand, there is a marked increase of the degree of orientation of the trans bonds in the amorphous phase. Furthermore, the orientation distribution of these conformers appears to be more centered along the draw direction. These results are in excellent agreement with those of Kaito et al.[37] obtained on roll-drawn high-density polyethylene by infrared and visible–ultraviolet dichroism. They have observed that the orientation function ($\langle P_2(\cos\theta)\rangle$) reaches a plateau at draw ratios higher than about 10 and that, during the roll-drawing process, the trans-rich sequences in the amorphous phase orient more readily in the draw direction than the gauche-rich sequences.

Backscattering Experiments. The backscattering (180°) geometry offers several advantages for orientation measurements by Raman spectroscopy. First, with this configuration, it is much easier to position the sample in the spectrometer, especially in the case of thick samples and of samples of irregular shapes. Second, it allows the

Table V
Orientation Distribution Coefficients of Polyethylene Obtained from Right-Angle (90°) and Backscattering (180°) Raman Measurements

frequency, cm^{-1}	λ	$\langle P_2(\cos\theta)\rangle$		$\langle P_4(\cos\theta)\rangle$	
		180°	90°	180°	90°
1130	7	0.79	0.75	0.49	0.56
	9.6	0.82		0.57	
	11.7	0.86	0.85	0.63	0.69

determination of the distribution of orientation in nonhomogeneous samples since the diameter of the focused laser beam on the sample has only approximately 200 μm. Finally, birefringence effects may be less important than for the right-angle scattering geometry because the scattered radiation comes from a small volume near the surface of the material. On the other hand, backscattering illumination limits the number of independent spectra that can be obtained so that it is not possible to solve eqs 7–11 only from backscattering measurements unless the sample is rotated along several directions.

However, once the values of the ratios α_1/α_3 and α_2/α_3 of the principal components of the Raman tensor are known from right-angle scattering measurements, the number of unknowns in eq 7–11 is reduced to three, and the system can be solved from backscattering spectra only. Since the intensity of the band due to the in-phase C–C stretching vibration at 1130 cm^{-1} is high enough to allow accurate measurements and since reliable values of α_1/α_3 and α_2/α_3 were obtained for this vibration, only the 1130-cm^{-1} band was analyzed for the backscattering experiments.

In order to obtain the three different $I_0\sum\alpha_{ij}\alpha_{pq}$ values required, it is no longer necessary to rotate the sample. If the angle γ is set to 0° (Figure 1b), it is possible to record the spectra $I_0\sum\alpha_{22}^2$, $I_0\sum\alpha_{32}^2$, and $I_0\sum\alpha_{33}^2$ (see the Experimental Section). In Figure 4, these three spectra are compared with those obtained by right-angle scattering. The excellent correspondence between the two sets of spectra indicates that accurate results can be obtained by backscattering illumination and that the depolarization due to birefringence effects is minimal.

Values of $\langle P_2(\cos\theta)\rangle$ and $\langle P_4(\cos\theta)\rangle$ obtained from the backscattering measurements on three samples of polyethylene roll-drawn at different draw ratios are presented in Table V. As can be seen, these results are in fairly good agreement with those obtained at right-angle scattering, the small discrepancies being due to inhomogeneity of orientation in the roll-drawn sheets. This was ascertained from measurements made on different areas on the samples. All values reported in Table V were calculated from spectra recorded in the center of the sheets where the maximum of homogeneity was observed. The results of Table V show that trans C–C bonds continue to reorient slightly parallel to the draw direction, even at a draw ratio of 11.7.

The backscattering spectra in the C–C stretching mode region recorded with the polarization direction of both the laser beam and the analyzer parallel to the draw direction ($I_0\sum\alpha_{33}^2$) are quite sensitive to the orientation of the polymer chains since the 1060- and 1130-cm^{-1} bands have $B_{2g} + B_{3g}$ and $A_g + B_{1g}$ symmetry, respectively. As seen in Figure 5, the relative intensity of the 1130-cm^{-1} band to that of the 1060-cm^{-1} feature increases significantly with the draw ratio and, therefore, provides an excellent probe of the orientation of the trans C–C bonds of polyethylene. In Figure 6, the h_{1130}/h_{1060} peak height intensity ratio is plotted as a function of the orientation coefficients $\langle P_2(\cos\theta)\rangle$ and $\langle P_4(\cos\theta)\rangle$ obtained from all

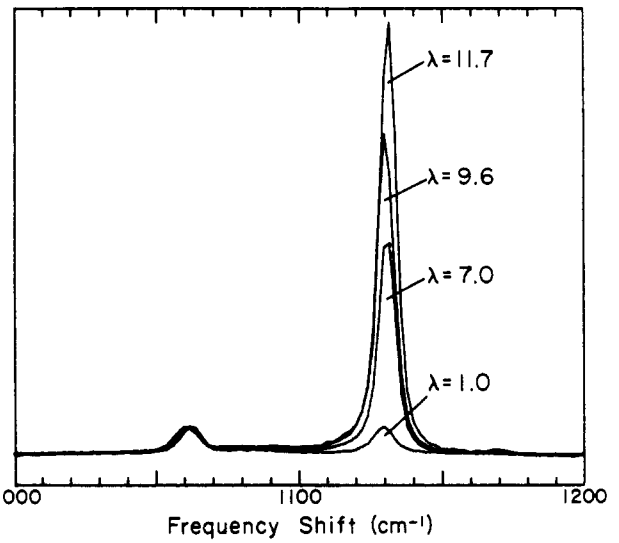

Figure 5. Effect of the draw ratio on the $I_0\sum\alpha_{33}^2$ backscattering Raman spectrum of polyethylene in the C–C stretching mode region.

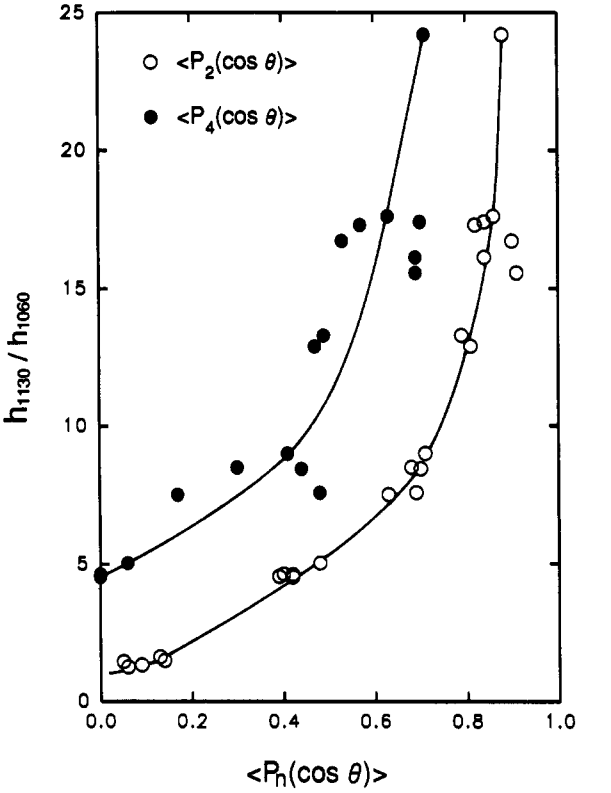

Figure 6. Correlations between the h_{1130}/h_{1060} intensity ratio in the $I_0\sum\alpha_{33}^2$ backscattering spectra and the $\langle P_2(\cos\theta)\rangle$ and $\langle P_4(\cos\theta)\rangle$ orientation coefficients.

backscattering experiments done on roll-drawn sheets. As can be seen, there is a fairly good correlation, although the data points are more scattered for $\langle P_4(\cos\theta)\rangle$ because this parameter is more sensitive to small intensity errors. Nevertheless, if the orientation averages $\langle P_2(\cos\theta)\rangle$ and $\langle P_4(\cos\theta)\rangle$ are smaller than 0.8, by using the calibration curves of Figure 6, it is possible to obtain rapidly good estimates of these averages from the $I_0\sum\alpha_{33}^2$ spectrum in the 1000–1200-cm^{-1} region only. This method should be particularly useful for the determination of the distribution of the orientation of C–C bonds with the trans conformation in thick processed samples of polyethylene. It should be mentioned that similarly good correlations were also obtained with extruded high-density polyethylene samples.

Conclusions

The results of the present study show that Raman spectroscopy can provide quantitative information about the molecular orientation of polyethylene. When the principal components of the Raman tensors are known, the backscattering geometry can be used to obtain rapidly good estimates of the orientation parameters $\langle P_2(\cos\theta)\rangle$ and $\langle P_4(\cos\theta)\rangle$. The results obtained show that, during the roll-drawing process, the extended chains in the crystalline phase are almost completely oriented at a draw ratio of 7 and that the trans C–C bonds in the amorphous phase orient more readily in the draw direction than the gauche defects.

Acknowledgment. We are grateful to Serge Alex and Claude-Paul Lafrance for several helpful discussions, to Josée Debigaré for the density measurements, and to Dr. R. Woodhams of the University of Toronto for providing the samples. This work was made possible through financial support from the Natural Sciences and Engineering Research Council of Canada, the Department of Education of the Province of Quebec (Fonds FCAR and Action structurante), and the Alcan Int. Co.

References and Notes

(1) Ward, I. M. *Structure and Properties of Oriented Polymers*; Applied Science Publishers: London, 1975.
(2) Ward, I. M. *Advances in Polymer Science*; Springer-Verlag: Berlin, 1985; Vol. 66, p 81–115.
(3) Jasse, B.; Koenig, J. L. *J. Macromol. Sci., Rev. Macromol. Chem.* **1979**, *C17*, 61.
(4) Cornell, S. W.; Koenig, J. L. *J. Appl. Phys.* **1968**, *39*, 4883.
(5) Snyder, R. G. *J. Mol. Spectrosc.* **1971**, *37*, 353.
(6) Bower, D. I. *J. Polym. Sci., Polym. Phys. Ed.* **1972**, *10*, 2135; *J. Phys. B: Atom. Mol. Phys.* **1976**, *9*, 3275.
(7) Purvis, J.; Bower, D. I. *Polymer* **1974**, *15*, 645.
(8) Maxfield, J.; Stein, R. S.; Chen, M. C. *J. Polym. Sci., Polym. Phys. Ed.* **1978**, *16*, 37.
(9) Satija, S. K.; Wang, C. H. *J. Chem. Phys.* **1978**, *69*, 2739.
(10) Robinson, M. E. R.; Bower, D. I.; Maddams, W. F. *J. Polym. Sci., Polym. Phys. Ed.* **1978**, *16*, 2115.
(11) Jasse, B.; Koenig, J. L. *J. Polym. Sci., Polym. Phys. Ed.* **1980**, *18*, 731.
(12) Purvis, J.; Bower, D. I. *J. Polym. Sci., Polym. Phys. Ed.* **1976**, *14*, 1461.
(13) Jarvis, D. A.; Hutchinson, I. J.; Bower, D. I.; Ward, I. M. *Polymer* **1980**, *21*, 41.
(14) Bower, D. I.; Jarvis, D. A.; Ward, I. M. *J. Polym. Sci., Polym. Phys. Ed.* **1986**, *24*, 1459.
(15) Gall, M. J.; Hendra, P. J.; Peacock, C. J.; Cudby, M. E. A.; Willis, H. A. *Spectrochim. Acta* **1972**, *28A*, 1485.
(16) Bailey, R. T.; Hyde, A. J.; Kim, J. J.; McLeish, J. *Spectrochim. Acta* **1977**, *33A*, 1053.
(17) Luu, D. V.; Abenoza, M.; Rault, J. *J. Phys. (Paris)* **1979**, *40*, 597.
(18) Masetti, G.; Abbate, S.; Gussoni, M.; Zerbi, G. *J. Chem. Phys.* **1980**, *73*, 4671.
(19) Strobl, G. R.; Hagedorn, W. *J. Polym. Sci., Polym. Phys. Ed.* **1978**, *16*, 1181.
(20) Snyder, R. G.; Scherer, J. R.; Peterlin, A. *Macromolecules* **1981**, *14*, 77.
(21) Wang, Y. K.; Waldman, D. A.; Stein, R. S.; Hsu, S. L. *J. Appl. Phys.* **1982**, *53*, 6591.
(22) Roe, R.-J. *J. Appl. Phys.* **1965**, *36*, 2024; *J. Polym. Sci., Polym. Phys. Ed.* **1970**, *8*, 1187.
(23) Treloar, L. R. G. *Trans. Faraday Soc.* **1954**, *50*, 881.
(24) Lafrance, C.-P.; Pézolet, M.; Prud'homme, R. E., unpublished results.
(25) Savoie, R.; Boulé, B.; Genest, G.; Pézolet, M. *Can. J. Spectrosc.* **1979**, *24*, 112.
(26) Schachtschneider, J. H.; Snyder, R. G. *Spectrochim. Acta* **1963**, *19*, 117.
(27) Gall, M. J.; Hendra, P. J.; Peacock, C. J.; Cudby, M. E. A.; Willis, H. A. *Polymer* **1972**, *13*, 104.
(28) Hendra, P. J.; Jobic, H. P.; Marsden, E. P.; Bloor, D. *Spectrochim. Acta* **1977**, *33A*, 445.
(29) Tasumi, M.; Shimanouchi, T. *J. Chem. Phys.* **1965**, *43*, 1245.
(30) Snyder, R. G. *J. Chem. Phys.* **1967**, *47*, 1316.
(31) Zerbi, G.; Magni, R.; Gussoni, M.; Holland-Moritz, K.; Bigotto, A.; Dirlikov, S. *J. Chem. Phys.* **1981**, *75*, 3175.
(32) Boerio, F. J.; Koenig, J. L. *J. Chem. Phys.* **1970**, *52*, 3425.
(33) Luu, D. V.; Cambon, L.; Lapeyre, C. *J. Raman Spectrosc.* **1980**, *9*, 172.
(34) Luu, D. V.; Cambon, L.; Lafont, R. *J. Raman Spectrosc.* **1980**, *9*, 176.
(35) Pitha, J.; Jones, R. N. *Can. J. Chem.* **1967**, *45*, 2347.
(36) Bower, D. I. *J. Polym. Sci., Polym. Phys. Ed.* **1981**, *19*, 93.
(37) Kaito, A.; Nakayama, K.; Kanetsuna, H. *J. Macromol. Sci., Phys.* **1987**, *B26*, 281.
(38) Glotin, M.; Mandelkern, L. *Colloid Polym. Sci.* **1982**, *260*, 182.
(39) Glotin, M.; Domszy, R.; Mandelkern, L. *J. Polym. Sci., Polym. Phys. Ed.* **1983**, *21*, 285.
(40) Clas, S.-D.; Heyding, R. D.; McFaddin, D. C.; Russell, K. E.; Scammell-Bullock, M. V.; Kelusky, E. C.; St-Cyr, D. *J. Polym. Sci., Polym. Phys. Ed.* **1988**, *26*, 1271.

Registry No. Polyethylene, 9002-88-4.